Soil Moisture Retrieval from Multi-Instrument and Multi-Frequency Simulated Measurements in Support of Future Earth Observing Systems

Amer Melebari[1], Sreeja Nag[2,3], Vinay Ravindra[2,3] and Mahta Moghaddam[1]

[1]*Ming Hsieh Department of Electrical and Computer Engineering*, *University of Southern California*, Los Angeles, CA, USA

[2]*NASA Ames Research Center*, Moffett Field, CA, USA

[3]*Bay Area Environmental Research Institute*, Moffet Field, CA, USA

amelebar@usc.edu

Abstract—**The majority of the soil moisture estimation algorithms using radars in the literature are for retrievals using a single instrument or not optimized for retrievals using multiple radars. A method for retrieving soil moisture using polarimetric radars at multiple frequencies is presented. The method uses a forward model and a hybrid local and global optimizer to retrieve soil moisture. Monte Carlo simulations of soil moisture retrieval using a maximum of four radars with different frequencies and incidence angles have been performed to assess the performance of the algorithm for various vegetation types and realistic instrument noise models. The simulation results show a mean unbiased root mean square error (ubRMSE) of less than 0.01 $\mathrm{m^3\,m^{-3}}$, and a mean bias less than 0.005 $\mathrm{m^3\,m^{-3}}$. The mean ubRMSE and bias values were quite small under the assumption that vegetation properties and surface roughness are known.**

Index Terms—**soil moisture, inverse-problem, remote-sensing, radar**

I. INTRODUCTION

In recent decades, multiple missions have been launched with the goal of estimating soil moisture on a regional and global scale. These include the National Aeronautics and Space Administration (NASA) Soil Moisture Active Passive (SMAP) mission [1], the European Space Agency (ESA) Soil Moisture and Ocean Salinity (SMOS) mission [2], and the Airborne Microwave Observatory of Subcanopy and Subsurface (AirMOSS) mission [3] among others. Furthermore, numerous algorithms have been developed to estimate soil moisture using microwave signals [4]–[7]. The majority of algorithms were designed to retrieve soil moisture value from a single instrument.

This paper focuses on retrieving surface soil moisture value from normalized radar cross section (NRCS) of multiple active radars. This work supports the development of future Earth observing systems, where multiple taskable space assets may be available for observing ground locations of interest based on science criteria, such as reducing the uncertainty of soil moisture knowledge at those particular ground points [8]. In our method, the soil moisture value is retrieved jointly

from the observations of all available instruments. The method is investigated for different vegetated terrains. The retrieval algorithm uses a multi-directional hybrid local and global optimization method based on simulated annealing and a forward scattering model.

The rest of the paper is organized as follows: Section II introduces the retrieval algorithm. The simulations setup is provided in Section III. The results and the discussions are presented in Section IV and Section V, respectively. Finally, the conclusion of this paper is given in Section VI.

II. RETRIEVAL ALGORITHM

The retrieval algorithm consists of an optimizer and a forward model. The multi-directional hybrid local and global optimization method based on simulated annealing [9] was used as an optimizer. This method has been proven to be faster than the standard simulated annealing in radar remote sensing applications [10]. The cost function integrates the normalized difference between the measured NRCS and the NRCS calculated by the forward model for all instruments and all polarizations. It is expressed mathematically as

$$f_{\text{cost}} = \sqrt{\sum_{i=1}^{N}\sum_{p=1}^{P_i} W[i,p]\left(\frac{\sigma^0_{\text{measured}}[i,p] - \sigma^0_{\text{fwd}}[i,p]}{\sigma^0_{\text{measured}}[i,p]}\right)^2} \quad (1)$$

where $\sigma^0_{\text{measured}}$ is the NRCS measured by the radar or simulated, σ^0_{fwd} is the NRCS calculated by the forward model, and N is the number of instruments. The quantity P_i is the number of measurements from instrument i. In our paper, this number corresponds to the number of polarizations. The parameter W is the weight of the measurement and is discussed in Section III.

The forward model is the Durden et al. radar backscattering model [11], but uses the soil dielectric constant model developed by Mironov et al. [12].

III. SIMULATION SETUP

Monte Carlo simulations were used to assess the retrieval algorithm performance. A maximum of four radars were

assumed to be available in the simulations; two were P-band, and the other two were L-band. All of the radars are quad-pol synthetic aperture radar (SAR) and have three operation modes. The center frequency, f_c, of the P-band and L-band radars are $435\,\mathrm{MHz}$ and $1.28\,\mathrm{GHz}$, respectively. The swath-width of the P-band radar was $50\,\mathrm{km}$, and the swath-width of the L-band radar was $25\,\mathrm{km}$. Each operation mode has a specific incidence angle, which gives a specific value of Noise equivalent sigma zero (NESZ) and a number of looks per km^2, N_{look}. The specifications of operating modes are given in Table I and Table II for the P-band and L-band radars, respectively. It is worth noting that the selection of radars' specifications is part of a novel design strategy for the next generation of Earth monitoring systems, whose description is outside the scope of this paper. The mapping between the radar specifications to the measurements metrics (NESZ, N_{look}) is obtained with the aid of the *InstruPy* Python package [8], [13]. This Python package contains models of various instruments (SAR, passive optical, radiometer) which maps instrument specifications to measurements metrics.

Five sites with distinct vegetation types have been studied. Table III shows the sites' names, vegetation types, and the International Geosphere-Biosphere Programme (IGBP) class of each vegetation type. The study was carried out in the wet period with soil moisture ranging between $0.16\,\mathrm{m}^3\,\mathrm{m}^{-3}$ and $0.3\,\mathrm{m}^3\,\mathrm{m}^{-3}$. The vegetation parameters of these vegetated terrains used in the forward model were presented in [4], [14], [15].

The simulated NRCS values were generated by the forward model with the addition of speckle noise [19] and system noise. It is expressed mathematically as

$$\sigma_{sim}^0 = \sigma_{forward}^0 \left(1 + \frac{0.523}{\sqrt{N_{look}}} w_1\right) + \kappa_p w_2 \qquad (2)$$

TABLE III
VEGETATION TYPES OF SIMULATION

Site name	Vegetation type	IGBP number
Metolius [16]	Evergreen needleleaf forest	1
Walnut Gulch [17]	Open shrublands	7
Tonzi Ranch [17]	Woody savannas	8
Yanco [18]	Croplands	12
Las Cruces [16]	Barren	16

where κ_p is the value of NESZ. Both w_1 and w_2 are independent white Gaussian random variables with zero mean and unity variance. The NRCS values of vv, hh, and vh polarization were used in the retrieval of soil moisture for all vegetation types except Barren. As the NRCS of cross polarization calculated by the forward model is zero, only the NRCS values of vv and hh polarization were used in the retrieval for the Barren case. For the quad-pol retrievals, the weighting W for the co-pol NRCS was $\frac{2}{5}$, and $\frac{1}{5}$ for the cross-pol NRCS. The co-pol measurements have a higher weight than the cross-pol measurement. For the case of retrievals using only the co-pol measurements, equal weight was given to both vv and hh polarization. Before the joint retrieval, the NRCS values with the same instrument type and incidence angle are averaged. Then, only the averaged NRCS value is used in the retrieval.

The simulations were done with ten Monte Carlo trials for the combinations of all unique operating modes. Each combination included at most the four radars in this study. Thus, soil moisture retrieval from a single radar or two radars up to four radars was considered. The total number of unique mode combinations for each vegetation type was 100. This is the number of combinatorics for all feasible variations of operation modes of the four instruments in this study. For each radar type, there are ten feasible combinations of operation modes. These include one of the radars is not active, or both are not active.

For comparison, a Monte Carlo simulation of soil moisture value retrieval using the SMAP radar specifications has been performed. Only the NRCS values of vv and hh polarization were used in the retrievals. The center frequency of SMAP radar is $1.257\,\mathrm{GHz}$, the incidence angle is $40°$, the N_{look} is 10, the NESZ is $-30\,\mathrm{dB}$, and the swath-width is $100\,\mathrm{km}$.

IV. RESULTS

The Monte Carlo simulations of soil moisture value retrievals from multiple instruments with multiple observations have been done for all of the unique mode combinations of the four instruments considered in this study. In addition, for the same vegetation parameters and soil moisture values, a Monte Carlo simulation using SMAP radar specifications has been done for comparison. The unbiased root mean square error (ubRMSE) and the bias were calculated for each mode combination and vegetation type using the definitions presented in [20]. The histograms of the ubRMSE and the bias for each vegetation type are shown in fig.1 and fig.2, respectively. The mean and the standard deviation values of ubRMSE and bias for each vegetation type are given in Table IV. Also, the performance of the retrievals using the SMAP radar specifications is provided in Table IV.

The performance of soil moisture retrievals using the proposed instruments was superior to the performance of retrieval using the SMAP radar specifications for all vegetation types. The mean values of the ubRMSE and the bias were quite small for all vegetation types. The difference in mean value between the various vegetation types, in this study, was insignificant.

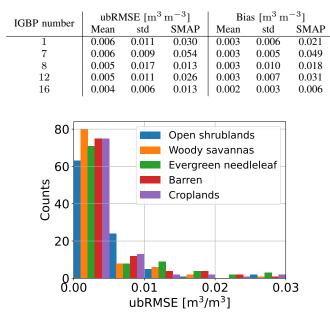| IGBP number	ubRMSE [$m^3\,m^{-3}$]			Bias [$m^3\,m^{-3}$]		
	Mean	std	SMAP	Mean	std	SMAP
1	0.006	0.011	0.030	0.003	0.006	0.021
7	0.006	0.009	0.054	0.003	0.005	0.049
8	0.005	0.017	0.013	0.003	0.010	0.018
12	0.005	0.011	0.026	0.003	0.007	0.031
16	0.004	0.006	0.013	0.002	0.003	0.006

Fig. 1. Histogram of ubRMSE of all the operating mode combinations. Note that the bars are narrow for clarity; the bar of each vegetation type should extend to the adjacent bars of the rest of the vegetation types.

However, there was a small variation in the standard deviation values. The retrievals from Woody savannas vegetation cover had the highest standard deviation of both ubRMSE and bias values. On the other hand, the retrieval from Barren vegetation type had the highest performance among the studied vegetation types.

Fig. 3 shows the mean ubRMSE values for the number of observations/instruments used in the retrieval. The use of two observations improved the retrieval performance for open shrublands vegetation type. The performance of the rest of the vegetation types in this study had a small change. We consider,
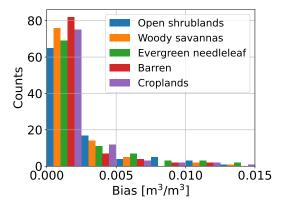

Fig. 2. Histogram of Bias of all the operating mode combinations. Note that the bars are narrow for clarity; the bar of each vegetation type should extend to the adjacent bars of the rest of the vegetation types.
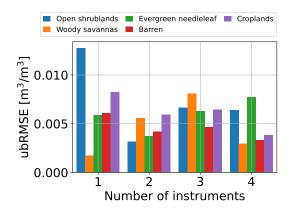

Fig. 3. Averaged ubRMSE values grouped to the number of instruments used in the retrieval.
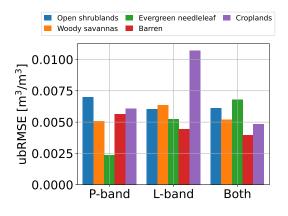

Fig. 4. Averaged ubRMSE values for retrievals from the P-band radars only, L-band radars only, and both.

in this study, a value of ubRMSE less than $0.005\,m^3\,m^{-3}$ insignificant, as this is negligible for practical purposes.

The averaged ubRMSE values for the retrievals grouped into retrievals using the P-band radar only, the L-band radar only, and both radars are presented in fig. 4. The figure shows that using only a P-band radar gives similar or better performance compared to using only an L-band radar in the retrieval of soil moisture value.

V. DISCUSSION

The Monte Carlo simulations showed that the proposed method of retrieving soil moisture using multiple instruments was able to retrieve soil moisture with high accuracy, as shown in Table IV. The proposed system of at most four radars had a higher quality of performance compared to the SMAP radar. This includes retrieving soil moisture using only a single instrument. For all vegetation types in this study, over $80\,\%$ of the modes combinations had an ubRMSE value less than or equal $0.01\,m^3\,m^{-3}$, as illustrated in fig. 1. This is a very low ubRMSE value, specially for wet regions.

The use of multiple independent observations improved the retrievals for some vegetation types. However, there was no noticeable difference between using two or more than two

observations in the retrieval. This was expected as soil moisture was the only unknown. The other surface and vegetation parameters were assumed to be known.

The retrievals using only the P-band radars had higher or similar performance compared to the retrievals using only the L-band radars. This was expected as P-band is less sensitive to vegetation and had higher measurement metrics, as shown in Table I. The measurements from the L-band radar is expected to improve the retrievals in the case of retrieving vegetation parameters with the soil moisture value, or when the P-band radar is not available.

The superior performance of soil moisture retrieval using the proposed system can be attributed to system specifications and the number of independent measurements. The performance of the retrievals exceeded the requirements of most existing systems and applications. In this study, only soil moisture value was retrieved. The other geophysical parameters, including surface roughness and vegetation water content, are assumed to be known. However, these other parameters are often unknown, or the accuracy with which they are known is low. The proposed system with this retrieval algorithm can be used in the future to estimate these parameters along with soil moisture, given that there are multiple observations assumed to be available.

The expected performance of each combination of operation modes can be used as a pre-processing step in a satellite constellation planner to inform the planner to select the optimum operation modes for the satellites [21].

VI. Conclusion

A soil moisture retrieval algorithm using multiple radar instruments, each with multiple polarizations, has been presented in this paper. Monte Carlo simulations of at most four instruments with multi-operation modes have been performed for various vegetation types. Both the speckle noise and the system noise were considered in the simulations.

The soil moisture retrieval results from the proposed system showed superior performance compared to retrievals using SMAP radar specifications. The mean ubRMSE and bias values were less than $0.01 \, \text{m}^3 \, \text{m}^{-3}$ and $0.005 \, \text{m}^3 \, \text{m}^{-3}$, respectively, and a standard deviation of less than $0.02 \, \text{m}^3 \, \text{m}^{-3}$, which are very small. We further note that resolution scale of the multi-instrument system vs. that of SMAP was not considered as a performance metric.

References

[1] D. Entekhabi, E. Njoku, P. O'Neill, M. Spencer, T. Jackson, J. Entin, E. Im, and K. Kellogg, "The soil moisture active/passive mission (SMAP)," in *International Geoscience and Remote Sensing Symposium (IGARSS)*, vol. 3, no. 1, 2008.

[2] Y. H. Kerr, P. Waldteufel, J.-P. Wigneron, J. Martinuzzi, J. Font, and M. Berger, "Soil moisture retrieval from space: the Soil Moisture and Ocean Salinity (SMOS) mission," *IEEE Transactions on Geoscience and Remote Sensing*, vol. 39, no. 8, pp. 1729–1735, 2001.

[3] M. Moghaddam, Y. Rahmat-Samii, E. Rodriguez, D. Entekhabi, J. Hoffman, D. Moller, L. E. Pierce, S. Saatchi, and M. Thomson, "Microwave Observatory of Subcanopy and Subsurface (MOSS): A mission concept for global deep soil moisture observations," *IEEE Transactions on Geoscience and Remote Sensing*, vol. 45, no. 8, pp. 2630–2643, 8 2007.

[4] A. Tabatabaeenejad, M. Burgin, X. Duan, and M. Moghaddam, "P-band radar retrieval of subsurface soil moisture profile as a second-order polynomial: First AirMOSS results," *IEEE Transactions on Geoscience and Remote Sensing*, vol. 53, no. 2, pp. 645–658, 2015.

[5] A. Etminan, A. Tabatabaeenejad, and M. Moghaddam, "Retrieving Root-Zone Soil Moisture Profile from P-Band Radar via Hybrid Global and Local Optimization," *IEEE Transactions on Geoscience and Remote Sensing*, vol. 58, no. 8, pp. 5400–5408, 8 2020.

[6] R. Akbar and M. Moghaddam, "A combined active-passive soil moisture estimation algorithm with adaptive regularization in support of SMAP," *IEEE Transactions on Geoscience and Remote Sensing*, vol. 53, no. 6, pp. 3312–3324, 6 2015.

[7] S. B. Kim, J. J. Van Zyl, J. T. Johnson, M. Moghaddam, L. Tsang, A. Colliander, R. S. Dunbar, T. J. Jackson, S. Jaruwatanadilok, R. West, A. Berg, T. Caldwell, M. H. Cosh, D. C. Goodrich, S. Livingston, E. Lopez-Baeza, T. Rowlandson, M. Thibeault, J. P. Walker, D. Entekhabi, E. G. Njoku, P. E. O'Neill, and S. H. Yueh, "Surface Soil Moisture Retrieval Using the L-Band Synthetic Aperture Radar Onboard the Soil Moisture Active-Passive Satellite and Evaluation at Core Validation Sites," *IEEE Transactions on Geoscience and Remote Sensing*, vol. 55, no. 4, pp. 1897–1914, 4 2017.

[8] V. Ravindra, R. Ketzner, and S. Nag, "Earth Observation Simulator (EO-Sim): An Open-Source Software for Observation Systems Design," *International Geoscience and Remote Sensing Symposium (IGARSS)*, vol. 2021-July, pp. 7682–7685, 2021.

[9] A. Etminan and M. Moghaddam, "Electromagnetic Imaging of Dielectric Objects Using a Multidirectional-Search-Based Simulated Annealing," *IEEE Journal on Multiscale and Multiphysics Computational Techniques*, vol. 3, pp. 167–175, 10 2018.

[10] A. Etminan, A. Tabatabaeenejad, and M. Moghaddam, "Retrieving Root-Zone Soil Moisture Profile from P-Band Radar via Hybrid Global and Local Optimization," *IEEE Transactions on Geoscience and Remote Sensing*, vol. 58, no. 8, pp. 5400–5408, 8 2020.

[11] S. L. Durden, J. J. Van Zyl, and H. A. Zebker, "Modeling and Observation of the Radar Polarization Signature of Forested Areas," *IEEE Transactions on Geoscience and Remote Sensing*, vol. 27, no. 3, pp. 290–301, 1989.

[12] V. Mironov, L. Kosolapova, and S. Fomin, "Physically and Mineralogically Based Spectroscopic Dielectric Model for Moist Soils," *IEEE Transactions on Geoscience and Remote Sensing*, vol. 47, no. 7, pp. 2059–2070, 7 2009.

[13] V. Ravindra and S. Nag, "Instrument Data Metrics Evaluator for Tradespace Analysis of Earth Observing Constellations," *IEEE Aerospace Conference Proceedings*, 3 2020.

[14] A. Tabatabaeenejad, M. Burgin, and M. Moghaddam, "Potential of L-band radar for retrieval of canopy and subcanopy parameters of boreal forests," *IEEE Transactions on Geoscience and Remote Sensing*, vol. 50, no. 6, pp. 2150–2160, 2012.

[15] R. Magagi, A. A. Berg, K. Goita, S. Belair, T. J. Jackson, B. Toth, A. Walker, H. McNairn, P. E. O'Neill, M. Moghaddam, I. Gherboudj, A. Colliander, M. H. Cosh, M. Burgin, J. B. Fisher, S. B. Kim, I. Mladenova, N. Djamai, L. P. B. Rousseau, J. Belanger, J. Shang, and A. Merzouki, "Canadian experiment for soil moisture in 2010 (CanEx-SM10): Overview and preliminary results," *IEEE Transactions on Geoscience and Remote Sensing*, vol. 51, no. 1, pp. 347–363, 2013.

[16] O. DAAC, "Soil Moisture Visualizer," Tennessee, USA, 4 2017.

[17] M. Moghaddam, A. Silva, D. Clewley, R. Akbar, S. Hussaini, J. Whitcomb, R. Devarakonda, R. Shrestha, R. Cook, G. Prakash, S. Santhana Vannan, and A. Boyer, "Soil Moisture Profiles and Temperature Data from SoilSCAPE Sites, USA," 2016. [Online]. Available: http://daac.ornl.gov/cgi-bin/dsviewer.pl?ds_id=1339

[18] A. B. Smith, J. P. Walker, A. W. Western, R. I. Young, K. M. Ellett, R. C. Pipunic, R. B. Grayson, L. Siriwardena, F. H. Chiew, and H. Richter, "The Murrumbidgee Soil Moisture Monitoring Network data set," *Water Resources Research*, vol. 48, no. 7, 7 2012.

[19] F. Ulaby and D. Long, *Microwave Radar and Radiometric Remote Sensing*. Ann Arbor: The University of Michigan Press, 2014.

[20] D. Entekhabi, R. H. Reichle, R. D. Koster, and W. T. Crow, "Performance metrics for soil moisture retrievals and application requirements," *Journal of Hydrometeorology*, vol. 11, no. 3, pp. 832–840, 6 2010.

[21] R. Levinson, S. Niemoeller, S. Nag, and V. Ravindra, "Planning Satellite Swarm Measurements for Earth Science Models: Comparing Constraint Processing and MILP Methods," in *International Conference on Automated Planning and Scheduling (ICAPS)*, 2022.